sustainability

MDPI

Article

Drying Performance of a Combined Solar Greenhouse Dryer of Sewage Sludge

Fatiha Berroug [1,2], Yassir Bellaziz [1,2], Zakaria Tagnamas [3], Younes Bahammou [1], Hamza Faraji [4,*], El Houssayne Bougayr [5] and Naaila Ouazzani [2,6]

1 Laboratory of Fluid Mechanic and Energy, Faculty of Sciences Semlalia, Cadi Ayyad University, Marrakech 40000, Morocco
2 National Center of Studies and Research on Water and Energy, Cadi Ayyad University, Marrakech 40000, Morocco
3 Team of Solar Energy and Aromatic and Medicinal Plants, ENS, Cadi Ayyad University, Marrakech 40000, Morocco
4 National School of Applied Sciences, Cadi Ayyad University, Marrakech 40000, Morocco
5 Laboratory of Engineering & Applied Technologies, Higher School of Technology, Sultan Moulay Slimane University, Beni Mellal 23000, Morocco
6 Laboratory of Water, Biodiversity and Climate Change, Faculty of Sciences Semlalia, Cadi Ayyad University, Marrakech 40000, Morocco
* Correspondence: hamza.faraji@uca.ac.ma

Abstract: The solar drying of sewage sludge in greenhouses is one of the most used solutions in wastewater treatment plants (WWTPs). However, it presents challenges, particularly in terms of efficiency and drying time. In this context, the present study explores the drying performances of an innovative Combined Solar Greenhouse Dryer (CSGD) for sewage sludge. The system integrates rock bed storage (RBS), a solar air collector (SAC), and a solar greenhouse dryer (SGD). A numerical model, developed using TRNSYS software, predicts the drying kinetics of sewage sludge through hourly dynamic simulations based on the climatic conditions of Marrakesh, Morocco. Experimental validation confirmed the accuracy of the model. The results reveal that integrating the SAC with the SGD during the day and the RBS with the SGD at night significantly enhances the drying efficiency of the sewage sludge. During daylight hours, the SAC generates hot air, reaching maximum temperatures of 64 °C in January and 109 °C in July. Concurrently, the outlet air temperature of the RBS rises notably during the day, corresponding to the charging phase of the storage unit. Moreover, during the night, the RBS air temperature exceeds ambient temperatures by approximately 7–16 °C in January and 11–37 °C in July. This integration leads to a substantial reduction in drying time. The reduction in sewage sludge water content from 4 kg/kg of dry solid (20% dry solid content) to 0.24 kg/kg of dry solid (80% dry solid content) is related to a decrease in the drying time from 121 h to 79 h in cold periods and from 47 h to 27 h in warm periods. The drying process is significantly enhanced within the greenhouse, both during daylight and nocturnal periods. The CSGD system proves to be energy-efficient, offering an effective, high-performance solution for sewage sludge management, while also lowering operational costs for WWTPs. This innovative solar drying system combines a thermal storage bed and a solar collector to enhance drying efficiency, even in the absence of sunlight.

Keywords: drying efficiency; greenhouse dryer; rock bed system; sewage sludge; solar collector; TRNSYS simulation moisture content

Citation: Berroug, F.; Bellaziz, Y.; Tagnamas, Z.; Bahammou, Y.; Faraji, H.; Bougayr, E.H.; Ouazzani, N. Drying Performance of a Combined Solar Greenhouse Dryer of Sewage Sludge. *Sustainability* **2024**, *16*, 9925. https://doi.org/10.3390/su16229925

Academic Editors: Olga De Castro Vilela and Chigueru Tíba

Received: 25 September 2024
Revised: 4 November 2024
Accepted: 11 November 2024
Published: 14 November 2024

1. Introduction

Population growth and the expansion of human activities have led to increased water consumption and wastewater discharge, resulting in greater pollution and straining treatment facilities. This situation affects aquatic ecosystems and poses risks to public

health. Wastewater treatment has become essential for our societies and represents a major challenge for sustainable development for future generations. The sewage sludge treatment takes up about two-thirds of the wastewater treatment plant budget, and the management of this sludge is crucial for environmental preservation [1,2].

Addressing the management and revalorization of this resource will be beneficial environmentally and economically [3]. Managing sewage sludge is essential to reduce its volume and transform it into valuable products. The primary methods for sewage sludge disposal encompass agricultural utilization and incineration. Lowering the moisture content of sewage sludge is essential for cost reduction during processing. Mechanical dehydration, which is a component of the wastewater treatment plant, typically yields a dry solids content ranging from 20% to 35%. However, achieving the necessary 80% to 90% dehydration, often required for subsequent treatment, typically necessitates thermal drying methods [4]. This process optimizes logistics efficiency and reduces transportation and storage costs.

Thermal drying processes for sewage sludge in wastewater treatment plants, such as belt dryers, rotary dryers, and fluidized bed dryers, use conventional heat sources to evaporate the water contained in the sewage sludge. Although effective, these processes have significant drawbacks in terms of energy consumption. They require a substantial amount of energy, leading to high operational costs and a significant carbon footprint. Additionally, they rely on fossil fuels, making them vulnerable to energy price fluctuations and environmental concerns. Hot-air drying is an employed primary sludge treatment technique where the rate of drying depends on a variety of factors, for instance, heating methods, air parameters, and sludge thickness [3–5]. In response to these challenges, the use of alternative methods such as solar drying is becoming increasingly popular, as it reduces energy consumption and costs while offering a more sustainable and ecological solution.

In Morocco, the annual potential production, coming from 84 existing WWTPs, is around 155,450 tons of dry sewage sludge. By 2030, and under the national program of sanitation, 108 other WWTPs will be operational [6]. The WWTP of Marrakesh (8.03° W, 31.62° N) is the first WWTP in Morocco that incorporates developed wastewater treatment, heat cogeneration, electricity, and biogas recovery [6]. The daily production of sewage sludge in this WWTP is around 140 tons. After mechanical dewatering, the dry solid content is about 20% and the dewatered sewage sludge is disposed for drying in an open sunshine area of 1.2 ha close to the municipal landfill. This kind of drying process depends on climatic conditions and necessitates a long time and immense surface to achieve the drying operation.

Morocco boasts considerable solar energy potential. The average yearly global radiation on a horizontal surface in Morocco is recorded at 5.3 kWh/m^2/day. Moreover, the total yearly duration of sunshine hours amounts to 2700 h in the northern regions and 3500 h in the southern regions. These conditions provide a solid foundation for harnessing solar energy, positioning Morocco as a key player in the renewable energy sector. Additionally, this abundance of solar radiation makes solar greenhouse drying an economical and effective solution for the dewatering of wastewater sewage sludge [7].

Greenhouse systems have garnered significant research attention due to the increasing demand for efficient sewage sludge treatment. In the literature, greenhouse solar dryers are the most suitable systems for drying sewage sludge. Studies show that CO_2 emissions for solar dryers range between 0.5 and 1.2 kgCO_2/kg of dry matter, depending on drying parameters [8]. In addition, they are cheap, easy to maintain, and have a high potential for pathogen removal [6]. The greenhouse is made with a transparent material that enhances the greenhouse effects and is equipped with ventilation and fans to control the humidity and the distribution of the inside drying air. In a recent study conducted by Khanlari et al. [9], an innovative approach to sewage sludge drying was examined, involving the design and analysis of a drying chamber equipped with a transparent cover. Both experimental and numerical investigations were conducted, revealing that the adoption of such a drying chamber led to a notable reduction in drying time. This study found that the average

specific energy consumption ranged between 1.77 and 2.86 kWh/kg, while the specific moisture extraction rate varied from 0.77 to 1.34 kg/kWh. Additionally, the levelized cost of heating for the system utilizing the drying chamber with a transparent cover was estimated to fall within the range of 1.7 to 2.0 USD cents/kWh [10]. Fantasse et al. [11] observed that high temperatures significantly reduce drying times. In their study, Masmoudi et al. [12] explored the efficacy of draining solar drying as an innovative approach for urban sanitation. Their research revealed that drying periods varied from 3 to 6 days during the summer and extended to 9 to 14 days throughout the winter season. By analyzing the drying rate curves, the researchers observed that increasing the air velocity led to a reduction in drying time. During the summer, only the falling rate period was evident, whereas in winter, the curves exhibited irregular patterns, deviating from typical drying kinetics. This analysis sheds light on the dynamics of draining solar drying and provides valuable insights into optimizing the drying process for sanitation applications. Chen et al. [13] introduced a system designed to address sewage sludge management by integrating various processes. This system involves drying wet sewage sludge using low-pressure steam, subsequently followed by the incineration of the dried sludge in a boiler. The incineration process generates steam, which is then utilized to power a steam turbine for electricity generation. This study's results indicate an impressive energy efficiency of up to 49.93%, alongside a competitive cost of electricity at 0.039 USD/kWh. Furthermore, the payback period is estimated at 13.63 years. This underscores the potential viability and economic feasibility of the proposed system for sewage sludge management [12]. In a recent study, Masmoudi et al. [14], conducted an experimental investigation on the drying kinetics of sewage sludge in a laboratory-scale solar drying bed, varying the sludge layer thickness in winter and summer. Their findings indicated that drying time increases with sludge thickness. Analysis of the moisture content and drying rate curves revealed that only the falling rate period was observed. This study also included empirical modeling of the drying behavior in this type of dryer. The findings of Svensson et al. [15] indicate significant potential for utilizing solar thermal energy as a supplementary source for sludge drying. However, due to the substantial emissions associated with intermediate sludge storage, the most advantageous approach is to employ multiple energy sources, enabling continuous operation of the drying process.

The solar greenhouse drying of sewage sludge stands out as an especially economical and promising solution, particularly for small- and medium-sized wastewater treatment plants (WWTPs) and developing countries. Moreover, solar greenhouses are relatively simple to construct and maintain, providing an accessible and sustainable solution for sludge treatment in contexts where financial and technical resources are limited. However, this method also has notable drawbacks. The primary challenge lies in its dependence on climatic and weather conditions. Indeed, the efficiency of solar drying varies according to the availability of sunlight, which can be problematic during cloudy or rainy periods. Additionally, solar drying does not function during the night, limiting the continuity of the dehydration process and potentially prolonging the time needed to achieve the desired moisture levels. It is crucial to consider these limitations. To maximize its effectiveness, it may be wise to combine this method with other energy sources, thereby mitigating climatic variations and ensuring continuous operation even in the absence of sunlight.

In this context, we contribute with this study by proposing a simple and cost-effective solution for solar energy storage, known as the rock bed storage system (RBS), to heat the air in the greenhouse during the night. The RBS functions as a sensible heat storage system, recognized for its affordability and widespread use. Typically, pebbles measuring 2 to 15 cm are utilized due to their high energy storage capacity, excellent thermal conductivity, durability, and cost-effectiveness. Solar energy is stored in the system during the diurnal period of the day and released into the greenhouse during the nocturnal period. Hence, our newly devised solar dryer system comprises three primary components: a rock bed storage system, a greenhouse, and a flat plate solar air collector. A numerical model was

constructed utilizing TRNSYS simulation and Fortran programming to forecast the effects of the integrated system on drying kinetics during both diurnal and nocturnal periods.

The outcomes of the simulation offer a valuable guideline for practical applications. This study aims to achieve several key objectives: assessing the influence of the storage system and the solar collector on the drying kinetics of sewage sludge in the solar greenhouse, improving the efficiency of sewage sludge drying throughout the day, and ensuring continuous drying even during periods without sunlight by leveraging the stored energy accumulated during daylight hours.

2. Materials and Methods

2.1. Material

Sewage sludge samples utilized in the experiment were sourced from the Marrakesh wastewater treatment plant. The measured initial dry moisture content of the samples was $80 \pm 2\%$. The total suspended solids were $20 \pm 2\%$. The volatile suspended solids were recorded at $55 \pm 5\%$ of dry matter and the sewage sludge pH was 7 ± 0.1. In this paper, dry solid content (DSC) is used instead of total suspended solids. DSC represents the mass ratio of dry matter to moist wet sewage sludge.

2.2. Modeling of the CSGD

As illustrated in Figure 1a, the SGD is made up only of a solar greenhouse, and the sewage sludge is spread inside the greenhouse. Through the greenhouse effect phenomenon which occurs inside the greenhouse, the temperature of the internal air increases, and as a result, drying of the sewage sludge inside the greenhouse occurs. For faster drying and to make the SGD more efficient, a flat plate solar air collector as an additional source of energy and a rock bed as a storage system for nocturnal drying were added to the SGD. Therefore, the Combined Solar Greenhouse Dryer (CSGD) (Figure 1b) for sewage sludge comprises three primary components: a rock bed storage unit, a flat plate solar air collector, and a solar greenhouse dryer.

Using the CSGD, drying occurs both during the day and night. From 8:00 am to 6:00 pm, solar radiation absorbed by the solar collector generates hot air. A portion of this hot air is directed into the solar greenhouse to improve drying throughout the day, while the remainder enters the rock bed from the top, transferring sensible heat to the pebbles. During the night, from 6:00 pm to 8:00 am, the thermal energy stored in the rock bed during the day is released to the greenhouse by circulating air through the storage bed. Heated air is then conveyed from the rock bed to the SGD via a pipe. Consequently, the drying time is reduced compared to a traditional SGD, where drying only occurs during daylight hours.

For this study, transient system simulation using TRNSYS software is employed to investigate the thermal behavior of the CSGD. TRNSYS is widely used by engineers and researchers worldwide to explore and validate new energy concepts. This software enables the specification of different system components and the establishment of connections between them using a flow diagram. Each component is characterized by numerous inputs, outputs, and parameters, with some outputs of one component serving as inputs for others. Although TRNSYS lacks a built-in component for simulating sewage sludge drying within a greenhouse climate, a Fortran program is developed to model the greenhouse solar dryer, which is then integrated with the selected TRNSYS components. In this study, the chosen system components include rock bed storage (type 10), a quadratic efficiency air collector (type 1b), a flow diverter (type 148a), weather data (type 15 2), and an online plotter (type 65c).

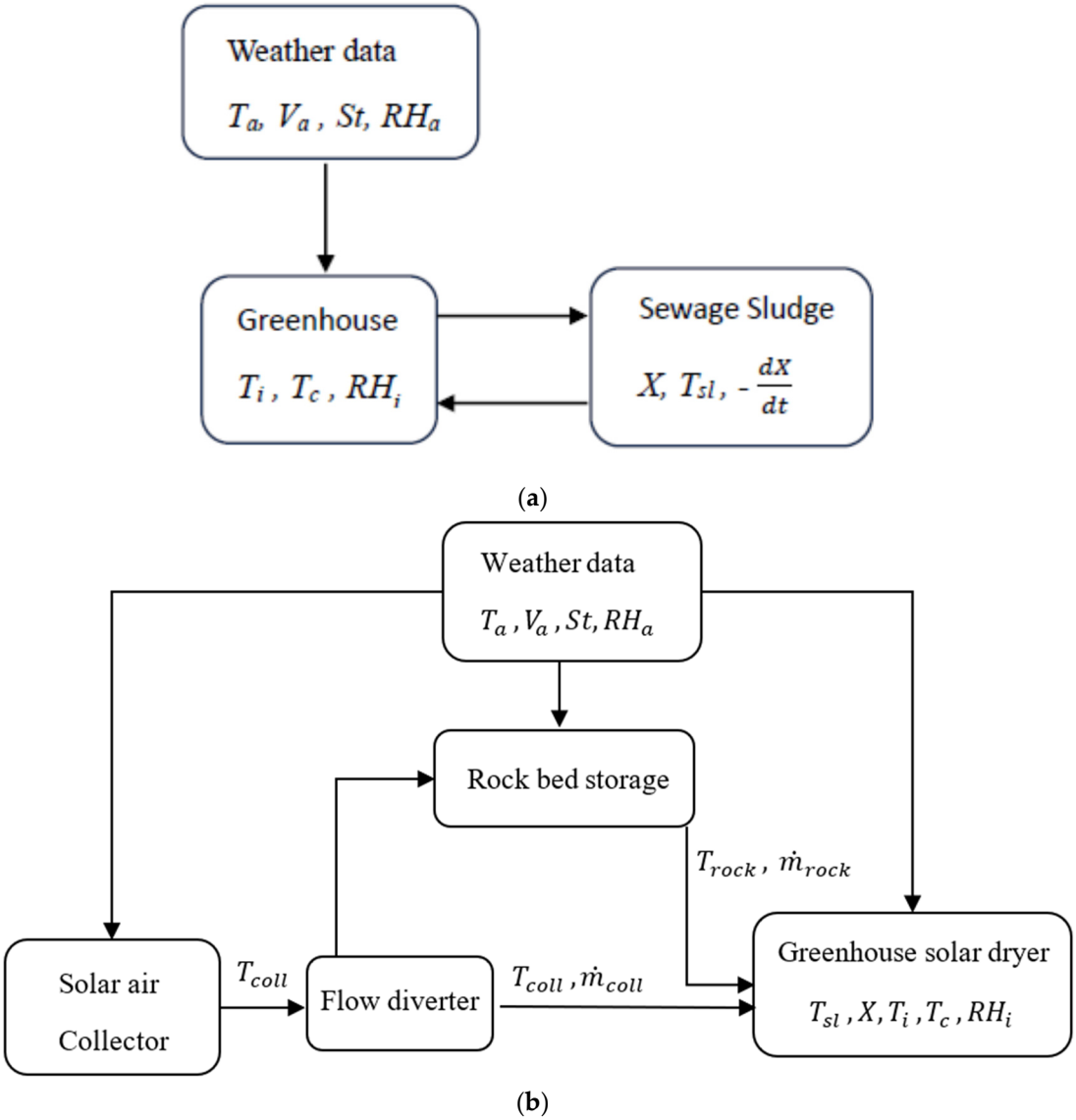

Figure 1. Schematic diagram of the SGD (**a**) and the CSGD (**b**).

2.3. Mathematical Formulation

In this section, mathematical formulation for the three main components of the CSGD is developed. Energy and mass balance equations are used to model each component.

2.3.1. Rock Bed Storage

Rock bed storage is an existing model in TRNSYS that is used in this study. The system can be elucidated by the equations governing heat transfer within a packed bed for fluid flow. The following assumptions are made [16]:

- Airflow through the bed is distributed uniformly.
- Neglected gradient temperature and axial conduction within the bed.
- Similar temperature of air and bed.

The partial differential equation describing both air and rock bed temperature is given by [16]

$$A\rho_r C_r \frac{dT_{rock}}{dt} = \dot{m}_{rock} C_i \frac{dT_{rock}}{dx} + UP(T_{rock} - T_a) \quad (1)$$

The attributes of rock bed storage (RBS) utilized in this investigation are outlined in Table 1.

Table 1. Parameters used for RBS.

Parameters	Values
Perimeter P	5 m
Length of rock bed	1.25 m
Cross-sectional area A	1.56 m^2
Specific heat of rock bed C_r	800 J $kg^{-1}K^{-1}$
Apparent rock bed density ρ_r	1800 kg m^{-3}
Loss coefficient U	0.84 $m^{-2}K^{-1}$

2.3.2. Flat Plate Solar Air Collector

The SAC used in this study is also a compound-validated model under TRNSYS software (Type 1b). The general equation for thermal solar collector efficiency used in TRNSYS is given by [17]

$$\eta = a_0 - a_1 \frac{(T_a - T_{coll})}{I_t} - a_2 \frac{(T_a - T_{coll})^2}{I_t} \quad (2)$$

where a_0, a_1, a_2 are, respectively, the optical efficiency, the linear heat loss coefficient, and the quadratic heat loss coefficient. The values of the SAC parameters for the simulation are summarized in Table 2.

Table 2. Parameters used for the SAC.

Parameters	Values
Area	9 m^2
Optical efficiency a_0	0.8
Linear heat loss coefficient a_1	3.6 W m^{-2} K^{-1}
Quadratic heat loss coefficient a_2	0.14 m^{-2} K^{-2}

2.3.3. Solar Greenhouse Dryer

To characterize the thermal dynamics of the SGD for sewage sludge, three elements must be considered in the thermal equilibrium: sewage sludge, internal air, and greenhouse cover (refer to Figure 2). The following hypotheses are made:

- The relative humidity and temperature of the internal air are presumed to be uniform.
- The temperature and moisture content of the sewage sludge are assumed to be uniform. Drying calculations are based on a thin-layer model.
- No radiant heat is absorbed by the greenhouse floor, which is entirely covered by sewage sludge.
- There is no condensation occurring within the greenhouse.

Energy balance of the internal air:

The energy balance equation for the internal air is expressed as follows:

$$\rho V_{gr} C_i \frac{dT_i}{dt} = Q^c_{s1,i} + Q^c_{c,i} + Q^c_{a,i} \quad (3)$$

where $Q^c_{sl,i}(W)$, $Q^c_{c,i}(W)$, and $Q^c_{a,i}(W)$ are, respectively, the convective heat transfers that occur between the internal air and three components: the sewage sludge, the cover, and the external air, which enters from the collector during the day and from the rock bed at night. Equation (3) can be written as

$$\rho V_{gr} C_i \frac{dT_i}{dt} = h^c_{s1,i} S_{s1} (T_{s1} - T_i) + h^c_{c,i} S_c (T_c - T_i) + h^c_{a,i} (T_{coll/rock} - T_i) \quad (4)$$

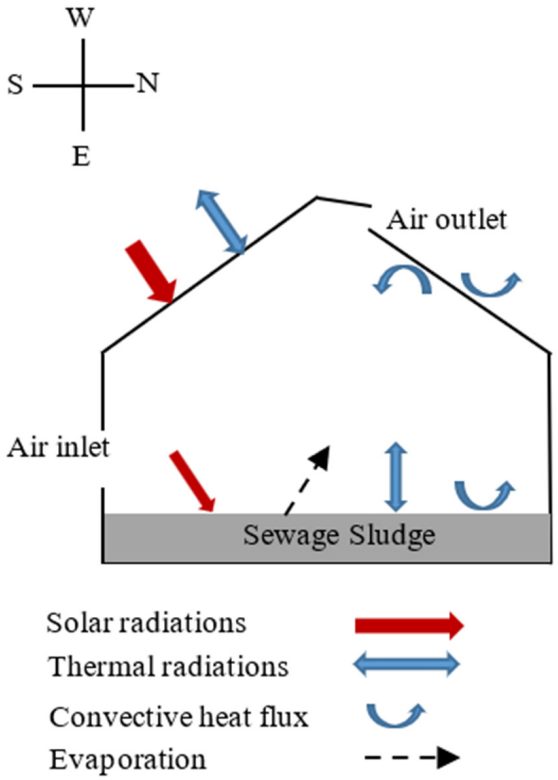

Figure 2. Heat and transfers within the SGD [18].

Mass balance of the internal air:
The mass balance equation for the internal air is expressed as follows:

$$\rho V_{gr} \frac{dw_i}{dt} = \dot{m}_{coll/rock}(w_a - w_i) + M_d\left(-\frac{dX}{dt}\right) \quad (5)$$

Energy balance of the dryer cover:
The energy balance equation for the cover is expressed as follows:

$$S_c C_c \frac{dT_c}{dt} = Q_c^s + Q_{a,c}^c + Q_{i,c}^c + Q_{sky,c}^r + Q_{sl,c}^r \quad (6)$$

where $Q_c^s(W)$ is the solar radiation absorbed by the cover. $Q_{a,c}^c(W)$ and $Q_{i,c}^c(W)$ are the convective heat transfers that occur between the cover and both the external and internal air of the greenhouse. Additionally, $Q_{sky,c}^r(W)$ and $Q_{sl,c}^r(W)$ represent the net thermal radiation exchanged between the cover and the sky, and between the cover and the sewage sludge, respectively.

Equation (6) can be written as

$$S_c C_c \frac{dT_c}{dt} = \alpha_{sc} Q_c + h_{a,c}^c S_c (T_a - T_c) + h_{i,c}^c S_c (T_i - T_c) + h_{sky,c}^r S_c \left(T_{sky} - T_c\right) + h_{sl,c}^r S_{sl} (T_{sl} - T_c) \quad (7)$$

where T_{sky} is the sky temperature (°C) which was calculated by

$$T_{sky} = 0.0552 \times (T_a + 273.16)^{1.5} - 273.16 \quad (8)$$

Energy balance of the sewage sludge:
The energy balance equation for the sewage sludge is expressed as follows:

$$m_{sl} C_{sl} \frac{dT_{sl}}{dt} = Q_{sl}^s + Q_{i,sl}^c + Q_{c,sl}^r - Q_{sl,i}^l \quad (9)$$

where $Q^{s}_{sl}(W)$ is the solar radiation transmitted to the greenhouse and absorbed by the sewage sludge. $Q^{c}_{i,sl}(W)$ is the convective heat transfer between the internal air and the sewage sludge. $Q^{r}_{c,sl}(W)$ is the net thermal radiation between the sewage sludge and the cover and $Q^{l}_{sl,i}(W)$ is the evaporation latent heat transfer between the internal air and the sewage sludge. Equation (9) can be rewritten as

$$m_{sl}C_{sl}\frac{dT_{sl}}{dt} = \alpha_{ssl}Q_{sl} + h^{c}_{i,sl}S_{sl}(T_i - T_{sl}) + S_c h^{r}_{sl,c}(T_c - T_{sl}) - M_d\left(-\frac{dX}{dt}\right)L_v \quad (10)$$

where $-\frac{dX}{dt}$ is the drying rate of sewage sludge. By applying the concept of the characteristic curve of drying [19], the sewage sludge drying rate can be expressed as

$$-\frac{dX}{dt} = \left(-\frac{dX}{dt}\right)_1 f(X_r) \quad (11)$$

where $f(X_r)$ represents the characteristic drying curve. In this investigation, the correlation established by [18] for sewage sludge generated in wastewater treatment plants located in Marrakesh is used:

$$f(X_r) = 2.28X_r - 1.35X_r^2 \quad (12)$$

where X_r is the reduced moisture ratio and is approximated by X/X_i. The first drying rate $\left(-\frac{dX}{dt}\right)_1$ is evaluated by using the energy balance of sewage sludge. The calorific capacity of sewage sludge C_{sl} is given by

$$C_{sl} = \frac{1}{1+X}C_{sld} + \frac{X}{1+X}C_w \quad (13)$$

where $Q_{sl}(W)$ and $Q_c(W)$ are the solar radiation incident on, respectively, the sewage sludge and the cover. They are estimated using the formulas established in a previously published study [18].

Convective and radiative heat transfer coefficients:

The convective and radiative heat transfer coefficients are given by

$$h^{c}_{a,i} = \dot{m}_{coll/rock}C_i \quad (14)$$

$$h^{r}_{sl,c} = \sigma\left(T_{sl}^2 + T_c^2\right) \times (T_{sl} + T_c)\left(\frac{1}{F_{sl,c}} + \frac{1}{\varepsilon_{sl}} - 1 + \frac{S_{sl}}{S_c}\left(\frac{1}{\varepsilon_{sl}} - 1\right)\right)^{-1} \quad (15)$$

$$h^{c}_{a,c} = 0.95 + 6.76.U_a^{0.49} \quad (16)$$

$$h^{r}_{sky,c} = \sigma\varepsilon_c\left(T_{sky}^2 + T_c^2\right)\left(T_{sky} + T_c\right) \quad (17)$$

$$h^{c}_{i,c} = \frac{Nu.K_a}{L_c}, h^{c}_{i,sl} = \frac{Nu.K_a}{L_{sl}} \quad (18)$$

Correlations based on the convection regime and the type of airflow within the greenhouse are employed to calculate the Nusselt number [18].

2.4. Numerical Simulation

The SGD model developed above relies on the principles of conservation of mass and energy. The resulting system comprises five differential equations, which are numerically solved using the fourth-order Runge–Kutta method implemented in FORTRAN. The input parameters of the model encompass the flow rate and temperature of hot air from the SAC and the RBS, external climatic conditions (solar radiation, ambient temperature, relative humidity, and airflow speeds of internal and external air), thermo-physical parameters of the sewage sludge, and the dimensional and thermo-physical parameters of the SGD. The parameters utilized in this computation are detailed in Table 3. The output parameters of

the model include the drying kinetics of the sewage sludge, internal relative humidity, and temperatures of the cover, internal air, and sewage sludge.

The thermal behavior of the SAC and the RBS is simulated by TRNSYS software, using the weather data of Marrakesh city with a time step of 1 h. The output parameters of these two components of the CSGD of sewage sludge are the outlet temperatures (T_{coll}, T_{rock}) and the outlet flowrates ($\dot{m}_{coll}$, $\dot{m}_{rock}$). They are used as input parameters for the numerical model developed, using Fortran to predict drying kinetics of sewage sludge in the SGD. The flow chart of the computation process is outlined in Figure 3.

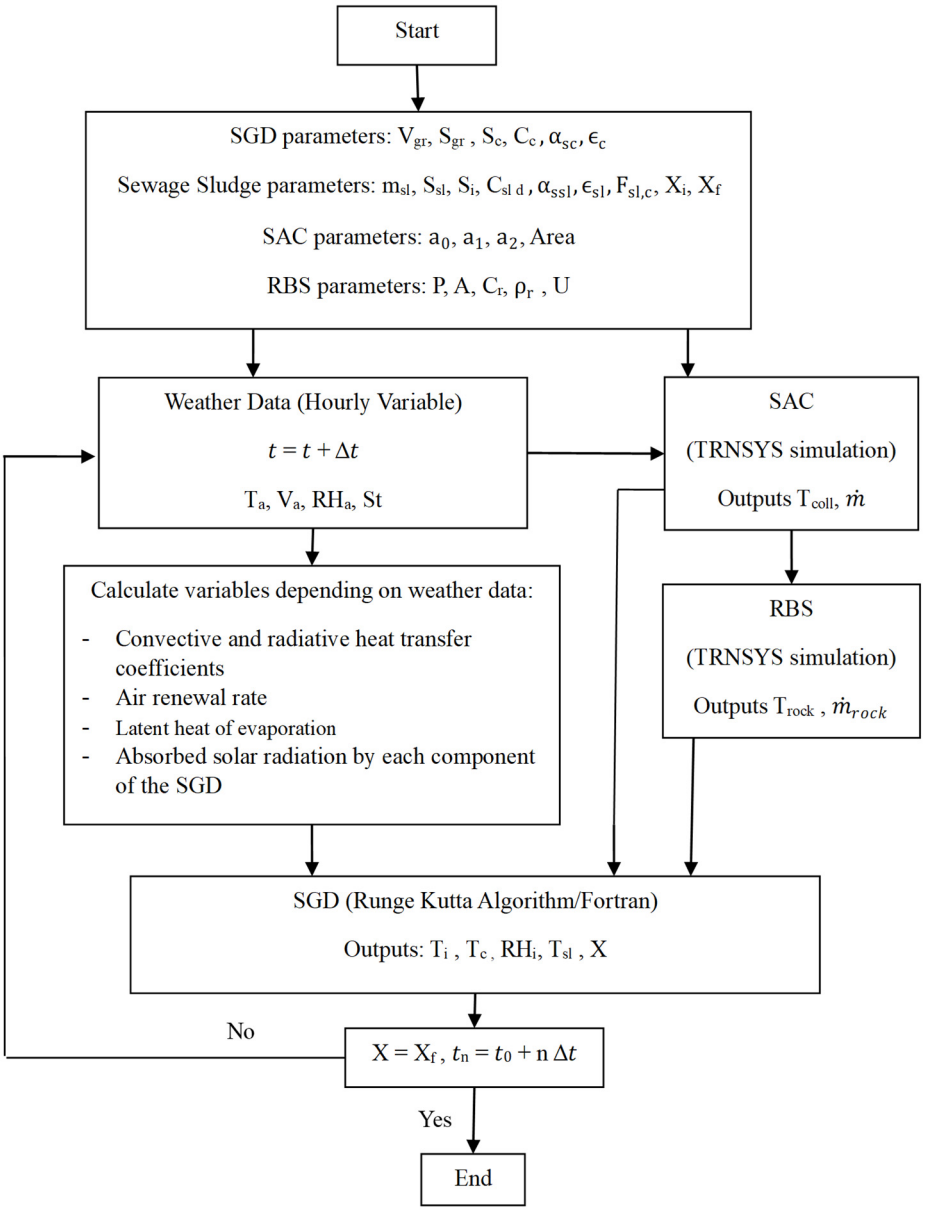

Figure 3. Flow chart of the computation process.

Table 3. Parameters used for the computation.

Parameters	Values
Sewage sludge	
m_{sl}, S_{sl}, S_i	192 kg, 24 m^2, 20%
$C_{sl\,d}$	1182 Jkg^{-1} K^{-1}
α_{ssl}, ϵ_{sl}, $F_{sl,c}$	0.8, 0.9, 1

Table 3. *Cont.*

Parameters	Values
Greenhouse	
V_{gr}, S_{gr}	57.6 m^3, 24 m^2
Cover	
S_c, C_c	68.76 m^2, 8000 W m^{-2} K^{-1}
α_{sc}, ϵ_c	0.8, 0.3

2.5. Energy Analysis of the CSGD

The utilization of the CSGD is different between the diurnal period and the nocturnal period. During the day, sewage sludge drying is assured by the energies provided to the SGD by solar radiation and the hot air generated from the SAC. And during the night, the energy supply to the SGD is provided from the RBS. Therefore, the energy supply (Ein) to the dryer is estimated by using Equation (19) during the day [20], while during the night, Equation (20) is used.

$$E_{in} = S_{gr} \times I + \dot{m}_{coll} \times C_i \times (T_{coll} - T_a) \quad (19)$$

$$E_{in} = \dot{m}_{rock} \times C_i \times (T_{rock} - T_a) \quad (20)$$

where I is the available solar radiations.

A part of the supplied energy E_{in} to the dryer is utilized to evaporate sewage sludge's moisture content. This amount of energy E_{out} is estimated as follows:

$$E_{out} = M_d \left(-\frac{dX}{dt} \right) L_v \quad (21)$$

The overall thermal efficiency of the CSGD is the ratio of the energy used to evaporate sewage sludge's moisture content to the total thermal energy supplied to the dryer. It is calculated using the following equation [20]:

$$\eta_{th} = \frac{\sum E_{out}}{\sum E_{in}} \times 100 \quad (22)$$

2.6. Model Validation

As previously mentioned, our Combined Solar Greenhouse Dryer (CSGD) for sewage sludge consists of three primary components. The SAC and the RBS are validated components within TRNSYS software [17]. To assess the validity of the third component, the SGD for sewage sludge, an experimental study was conducted using a solar sewage sludge pilot dryer situated in Marrakesh city [6], specifically at the National Centre for Studies and Research on Water and Energy (CNEREE). The pilot dryer measures 60 cm in width and 160 cm in length, with a greenhouse height of 50 cm at the gutter level and 80 cm at the span level. The greenhouse cover comprises a 1 cm thick transparent polycarbonate sheet. Its orientation is east–west to maximize exposure to solar radiation.

Sludge samples are spread inside the greenhouse on a plate of stainless steel (25 cm length, 20 cm width, and 2.5 cm height). Each plate contains 650 g of sewage sludge. The drying kinetics of the sewage sludge samples are evaluated using the moisture content by measuring the sample's weight every hour. The surrounding meteorological data of the greenhouse are obtained from the weather station Davis Vantage Pro 2 installed on the CNEREE roof. Figure 4a,b illustrate the outside weather conditions for the period of experimentation. The results show that a ratio of the dry solid content of 90% and 98% is reached in 78 and 96 drying hours, respectively.

Numerical simulations of the SGD using the experimental conditions mentioned above were conducted. The Mean Relative Error (MRE) and the Root-Mean-Squared Error (RMSE)

are used to evaluate the accuracy of the model in this study. The mathematical expression of these errors is given by

$$\text{MRE } (\%) = \frac{100}{N} \sum_{i=1}^{N} \frac{\left| X_{exp,\,i} - X_{sim,\,i} \right|}{X_{exp,\,i}}$$

$$\text{RMSE } (kg/kg) = \sqrt{\frac{1}{N} \sum_{i=1}^{N} \left(X_{exp,\,i} - X_{sim,\,i} \right)^2}$$

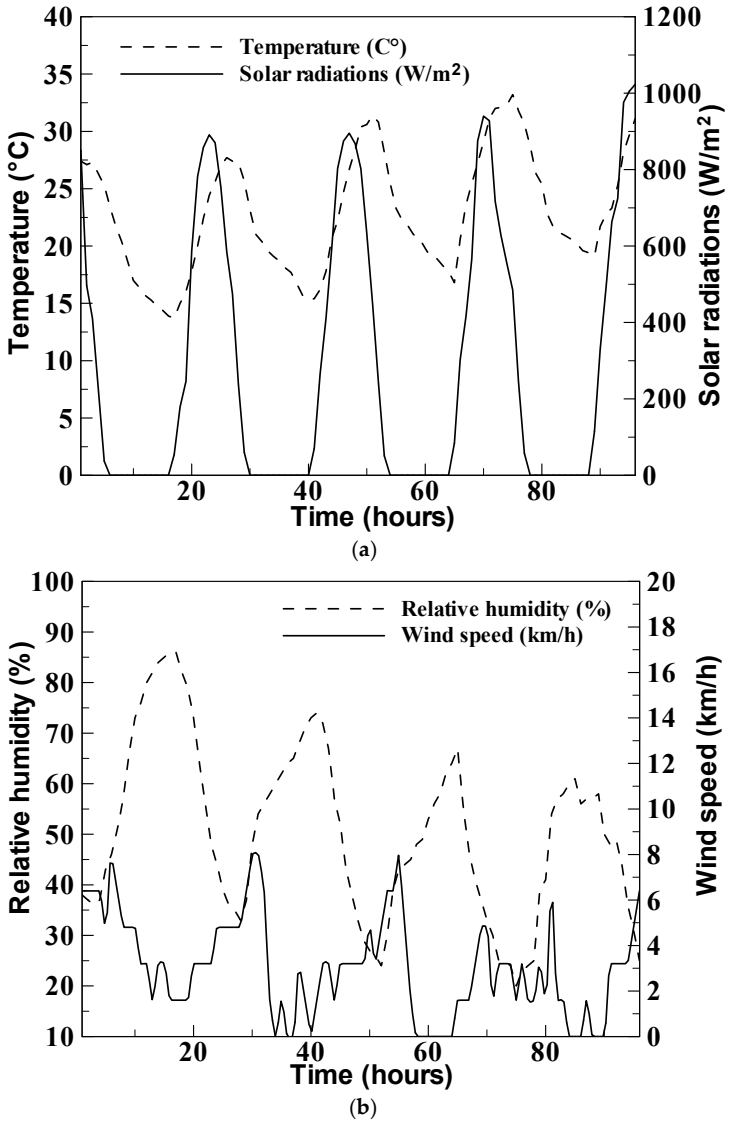

Figure 4. (**a**) Ambient temperature and global solar radiations of the experimental period. (**b**) Relative humidity and wind speed of the experimental period.

Figure 5 depicts the variation in both experimental and numerical moisture content of sewage sludge. The comparison illustrates a favorable agreement between the two models. The Mean Relative Error (MRE) and the Root-Mean-Square Error (RMSE) are determined to be 2.9% and 0.017 kg/kg, respectively. Discrepancies between measured and simulated moisture content can be attributed to the utilization of correlations for estimating heat and mass transfer coefficients, simplifying assumptions incorporated in the numerical model, and measurement errors. This allows us to consider our model suitable to simulate drying kinetics of sewage sludge under different operation conditions.

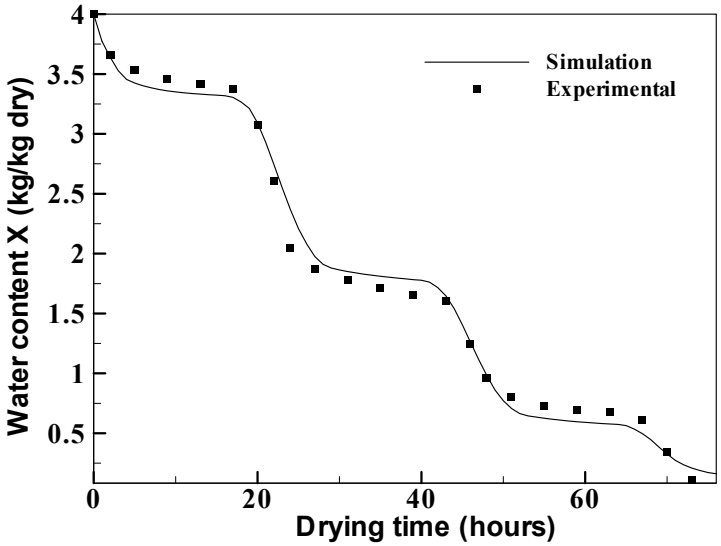

Figure 5. Comparison between the predicted and measured moisture content.

3. Results and Discussions

3.1. Meteorological Data and Thermal Performance of the SAC and the RBS

Figure 6a,b represent the variation in relative humidity, ambient temperature, wind velocity, and global solar radiations throughout the year in Marrakesh (8.03° W, 31.62° N). As seen in these figures, July and August can be considered the hot period in the year. In fact, maximum solar radiations (1050 W/m^2) and ambient temperature (40 °C) are detected in these months. Minimum relative humidity is also registered in this period (20%). Furthermore, December and January can be considered the cold period in the year. Minimum solar radiations (400 W/m^2) and ambient temperature (5 °C) are recorded in this period with a maximum relative humidity (100%).

Figure 7a,b show the hourly variation in the outlet air temperature in the SAC and the RBS during the last week of January and the third week of July. These two weeks are chosen to illustrate the thermal behavior of the SAC and the RBS in cold and hot periods in Marrakesh. The variation in temperature with time is periodic.

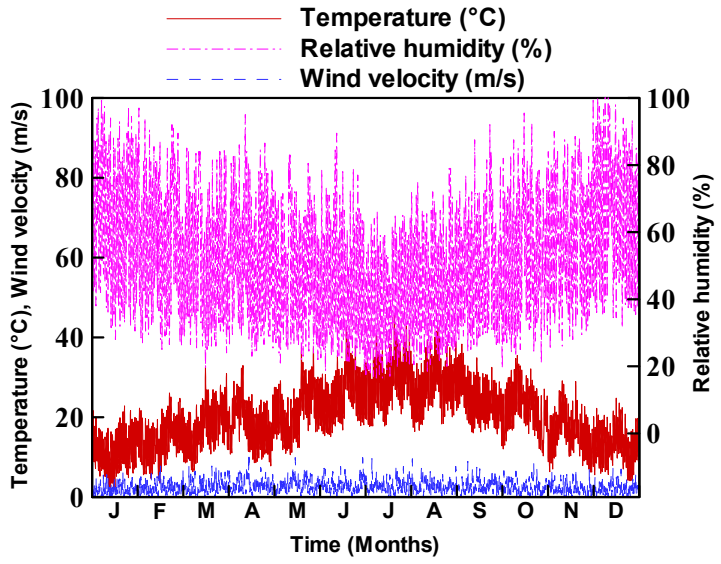

(**a**)

Figure 6. *Cont.*

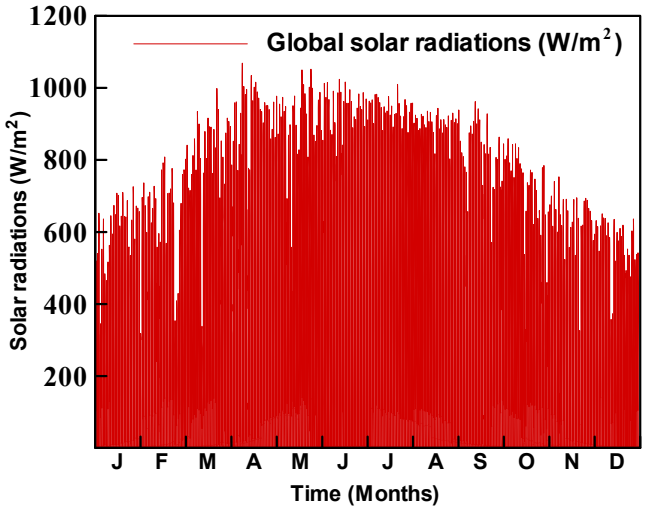

(**b**)

Figure 6. (**a**) Variation in temperature, relative humidity, and wind velocity throughout the year in Marrakesh. (**b**) Variation in global solar radiations throughout the year in Marrakesh.

During daylight hours, typically from 8:00 a.m. to 6:00 p.m., the SAC generates hot air, reaching temperatures of up to 64 °C in January and 109 °C in July. Concurrently, the air temperature within the RBS steadily rises throughout the day, peaking around 5:00 p.m. to 6:00 p.m., marking the charging phase of the storage unit. This increase in temperature is attributed to the influx of hot air supplied by the SAC and injected into the RBS during daytime operation. Subsequently, during the nighttime, approximately from 6:00 p.m. to 8:00 a.m., representing the discharge phase of the RBS, the outlet air temperature remains notably higher than the ambient temperature, ranging from 7 to 16 °C higher in January to 11–37 °C higher in July (Figure 7a,b). Consequently, the hot air provided by the SAC during the day and by the RBS during the night to the SGD enhances drying efficiency within the greenhouse. Similar findings were reported by [21], indicating that the utilization of a storage unit helps maintain higher air temperatures within the solar greenhouse, typically by approximately 7.5 °C compared to ambient temperatures during the nighttime. Additionally, the relative humidity within the drying chamber significantly decreases, lowered by around 18.6% compared to ambient relative humidity after sunset. Dryers equipped with storage units achieve a substantial 95% reduction in moisture content within 30 h [21].

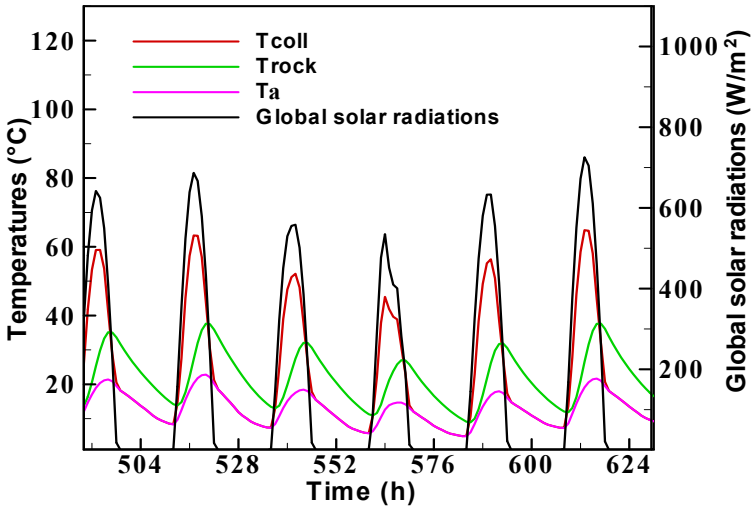

(**a**)

Figure 7. *Cont.*

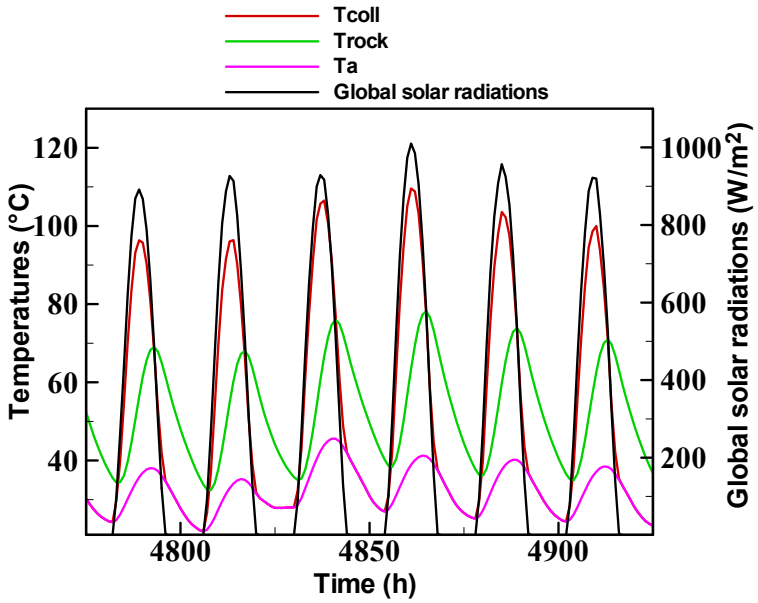

(**b**)

Figure 7. (**a**) Variation in the outlet air temperature at the SAC and the RBS during the last week of January in Marrakesh. (**b**) Variation in the outlet air temperature at the SAC and the RBS during the third week of July in Marrakesh.

3.2. Thermal Performance of the SGD (Without SAC and RBS)

This section examines the drying efficiency of the SGD without supplementary heated air circulation (SAC and RBS). The drying simulation on the SGD started on January 21 at 12 p.m. The initial moisture content is 4 kg water/kg dry basis, which corresponds to a dry solid content of 20%. The sewage sludge was dried to a moisture content of 0.24 kg water/kg dry basis, which corresponds to a dry solid content of 80%.

Figure 8 depicts the temperature variations in the system components—namely the cover, sewage sludge, and internal air—over the final week of January in Marrakesh. Upon analysis of this figure, it becomes evident that the internal air temperature within the greenhouse (air-drying) rises as it absorbs solar radiation, surpassing the external air temperature. As illustrated in Figure 8, the temperature contrast in the air between the inside and outside of the greenhouse peaks at 8 °C on the initial drying day and 30 °C on the concluding drying day. These increments are attributed to the greenhouse effect, which typically involves convective and radiative physical processes [18].

Despite receiving a significant portion of solar radiation, the cover temperature remains relatively close to the internal air temperature. This can be attributed to energy losses through convective and radiative exchanges with the external environment.

The sewage sludge temperature experiences a rapid increase compared to the internal air temperature. Notably, the temperature disparity between the sewage sludge and external air reaches 14 °C on the initial drying day and escalates to 50 °C on the final drying day. This discrepancy is primarily attributed to the relatively high solar radiation absorbed by the sewage sludge. Furthermore, as the water content in the sludge decreases after the second drying day, the evaporation rate diminishes significantly. Consequently, the energy required for the phase change of water from liquid to vapor in the sewage sludge decreases substantially, resulting in an overheated sewage sludge (reaching 70 °C on the last drying day). Additionally, during the night, the temperature of the system components decreases, occasionally dropping a few degrees below the external air temperature. This decline in temperature is attributed to nocturnal heat losses from the polyethylene-covered greenhouse. Similar observations have been reported by other researchers investigating solar greenhouse dryers [21–24].

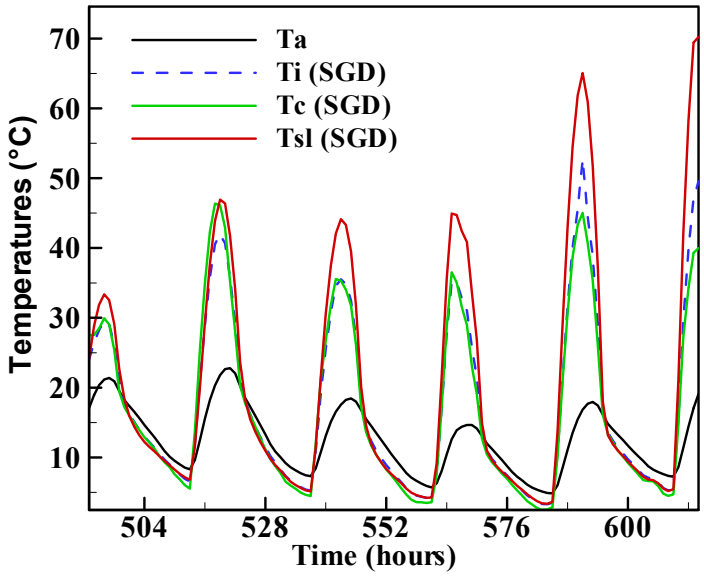

Figure 8. Variation in the temperature of internal air, greenhouse cover, and sewage sludge during the last week of January in Marrakesh.

Figure 9 illustrates the evaporated flux (drying rate) per sewage sludge surface as a function of the moisture content of sewage sludge, commonly referred to as Krischer's curve [3,23]. This curve aids in identifying different phases of the drying process [23], and the number of phases is contingent upon the material being dried, the type of dryer, and the operational conditions. Typically, under constant drying conditions, this curve consists of three primary segments. Initially, there is a constant drying rate as free water is removed. Subsequently, one or two falling rate phases follow, during which interstitial and surface water are eliminated. Finally, there is a brief period where bound water is removed, leading to the attainment of moisture content equilibrium. However, in the case where the dryer is a solar greenhouse, the operating conditions are variables and the drying rate depends on the greenhouse environment, which is a function of the meteorological data [18]. Consequently, the classical segments of Kricher's curves are not evident. Furthermore, since mechanical dewatering, a standard procedure in wastewater treatment plants, removes all free water from the sewage sludge [5], the constant drying rate is absent. Confirming this, [25] noted the absence of a constant drying rate for dewatered sewage sludge. The drying simulation presented herein was conducted for dewatered sewage sludge, with an initial dry solid content of 20%, which is below the critical moisture content. The results depicted in Figure 9 suggest that the drying rate is periodic, with minimal values near or equal to zero at night and maximal values during the daytime, exhibiting a significant variation between the beginning and the end of the drying process [3].

3.3. Thermal and Drying Performances of the CSGD

The temporal variations in internal air temperature and sewage sludge temperature during the drying process for the final week of January and the third week of July in Marrakesh are illustrated in Figure 10a,b and Figure 11a,b, respectively, for both the CSGD and the SGD.

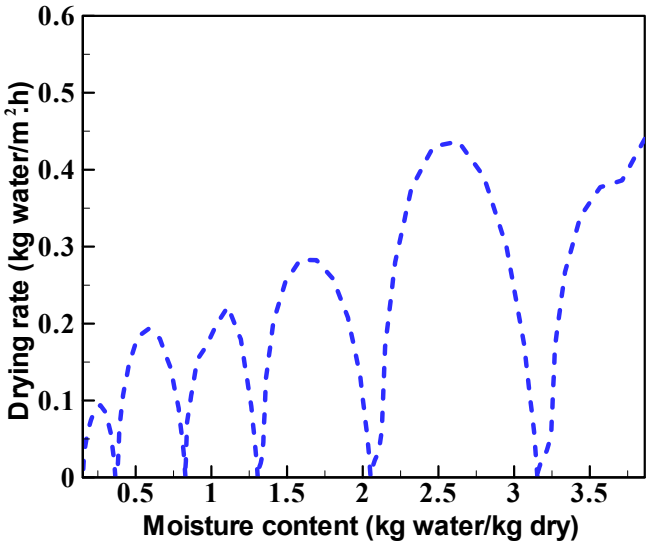

Figure 9. Variation in the drying rate of sewage sludge with the moisture content variation during the last week of January in Marrakesh.

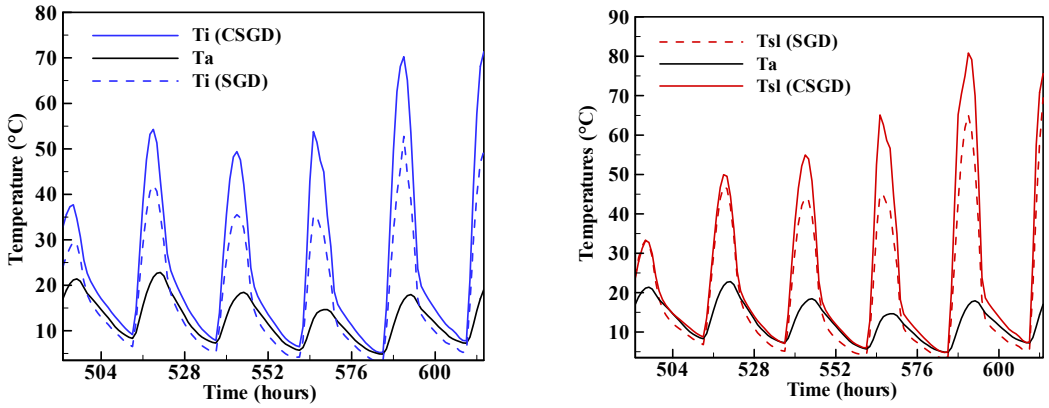

Figure 10. Variation in internal air temperature (**a**) and sewage sludge temperature (**b**) during the drying process for the last week of January in Marrakech.

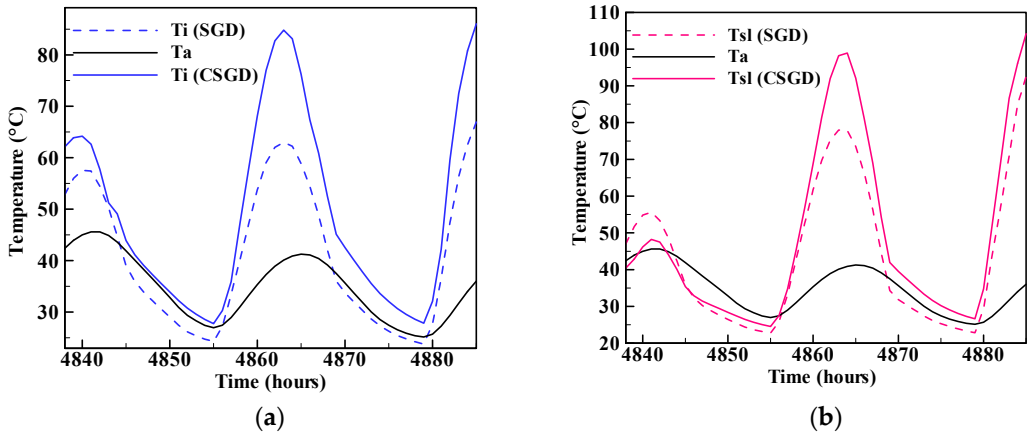

Figure 11. Variation in internal air temperature (**a**) and sewage sludge temperature (**b**) during the drying process for the third week of July in Marrakesh.

The analysis of these figures reveals that the internal air temperature of the greenhouse rises significantly when exposed to solar radiation, surpassing the temperature of the

external air. In addition, internal air and sewage sludge temperatures are significantly enhanced in the CSGD compared to SGD. Indeed, the diurnal temperature difference between SGD and CSGD reaches a maximum value of 18 °C for internal air and 19 °C for sewage sludge during cold periods. During warm periods, the diurnal temperature difference for SGD and CSGD reaches 20 °C for internal air and 21 °C for sewage sludge. This is attributed to the heat supplied to the greenhouse by the SAC during the day. Similarly, the nocturnal temperature difference reaches 5 °C for internal air and sewage sludge during cold periods. It also reaches, during warm periods, 8.5 °C for internal air and 7 °C for sewage sludge. This temperature elevation is due to the warm air provided by the RBS to the greenhouse during the night.

Figure 12a,b, respectively, illustrate the evolution of water content and drying rate of sewage sludge (evaporative power) during the last week of January and the third week of July in Marrakesh.

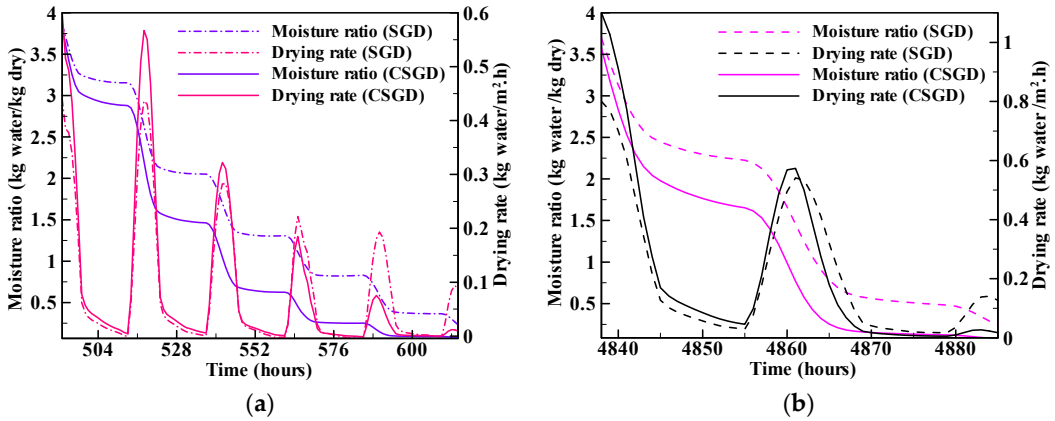

Figure 12. Variation in moisture content and drying rate of sewage sludge during (**a**) the cold period (January) and (**b**) the warm period (July).

As depicted in Figure 12a,b, the reduction in moisture content is not uniform. It is evident that during the day, there is a significant decrease in moisture content, primarily due to the solar radiation absorbed by the sewage sludge and the greenhouse effect. However, during the night, the change in moisture content is not as pronounced. Furthermore, it is observed that the variation in moisture content from the initial drying day is greater than that observed on the final drying day. Specifically for the SGD, the moisture content decreased from 3.17 to 2.07 kg water/kg dry basis on the second drying day, whereas it only decreased from 0.57 to 0.24 kg water/kg dry basis on the last drying day. This discrepancy is attributed to the reduction in the amount of evaporated water in the sewage sludge, a trend that is supported by the drying rate curve (Figure 8). The average daily drying rate is 0.24 kg water/m^2 h for the second drying day, and it is 0.08 kg water/m^2 h for the last drying day. Therefore, drying kinetics is important at the beginning of drying and decreases with time [24,25]. By using a greenhouse as a solar dryer for sewage sludge, drying occurs only in the daytime period, and 121 h is required for drying sewage sludge in the cold period of Marrakesh (Figure 11a).

In addition, the results indicate that the evaporative capacity is higher, and the drying time is shorter for the CSGD. Specifically, the time required to decrease the water content from 4 kg/kg dry solid (DSC of 20%) to 0.24 kg/kg dry basis (DSC of 80%) decreases from 121 h to 79 h in colder periods and from 47 h to 27 h in warmer periods. Consequently, the integration of the SAC during the day in the greenhouse and the RBS during the night has expedited the drying process by an average of two days in colder periods and one day in warmer periods in the climate of Marrakesh. This acceleration can be attributed to the increase in drying air temperature inside the greenhouse.

To analyze the drying performance of both the SGD and the CSGD systems, Table 4 presents the average diurnal and nocturnal drying rates at the onset of the drying process

(first day), a critical period when this rate is particularly important [23]. As the water content of the sewage sludge decreases, the diffusion of vapor into the air diminishes (Figure 12a,b) [24,25]. Based on the findings shown in Table 4, it is evident that the drying rate of sewage sludge in the CSGD, in comparison with the SGD, is enhanced by 0.13 kg of water/m^2.h during the cold period and by 0.3 kg of water/m^2.h during the warm period. Additionally, the nocturnal drying rate experiences an increase of 0.01 kg of water/m^2.h during the cold period and 0.083 kg of water/m^2.h during the warm period.

Table 4. Average drying rates for SGD and CSGD.

Drying Rate (kg Water/m^2.h)	SGD		CSGD	
	Day	Night	Day	Night
Cold period	0.28	0.021	0.41	0.031
Warm period	0.50	0.057	0.80	0.14

It should be noted that the drying process is enhanced in the CSGD both during the day and the night. The improvement is more pronounced during warm periods. However, the enhancement of nocturnal drying remains moderate. This is attributed to the surface area utilized for rock bed storage, which is 1.25 m^2 for a greenhouse area of 24 m^2. Increasing the surface area of the rock bed storage will certainly enhance nocturnal drying in the greenhouse. Thus, the surface area of the rock bed can be determined based on the desired drying rate during the night. The overall efficiency of the CSGD is found as 22% during the warm periods and 18% during the cold periods. The results are very interesting compared to other drying systems [20]. And a comparison between the CSGD and other sludge treatment systems revealed that the CSGD reduces drying time by 20–25%, offering a faster and more eco-efficient alternative to conventional thermal processes [10,26–28].

In addition, the use of the CSGD, due to its increased efficiency, could enable an energy cost reduction of 15–20% compared to systems using only conventional energy, especially for small- and medium-sized plants where energy cost is a major constraint. This presents a strong economic argument for its implementation.

4. Conclusions

In this study, a TRNSYS model of a greenhouse system was developed to evaluate the effect of a thermal storage unit and a solar air collector on sewage sludge drying rates under varied climatic conditions. The model shows strong agreement with experimental data, achieving a Mean Relative Error of 2.9% and RMSE of 0.017 kg/kg. During storage charging, outlet air temperatures from the regenerative heat storage system exceed ambient temperatures by 7–16 °C in January and 11–37 °C in July, significantly improving drying. This setup reduces drying time by two days in colder periods and one day in warmer periods, indicating its suitability for large-scale wastewater treatment applications and sustainable resource management. This novel approach represents a step forward in optimizing eco-friendly drying processes, particularly for developing countries. Future research could explore adjustments to the storage bed parameters to further enhance nighttime performance, as well as the evaluation of alternative materials for the solar collector to maximize energy efficiency. In addition, the next steps for this research include optimizing the storage bed and further evaluating its thermal storage capacity, particularly for more pronounced seasonal variations.

Author Contributions: Conceptualization, F.B. and H.F.; Methodology, F.B., Y.B. (Yassir Bellaziz), Z.T., Y.B. (Younes Bahammou) and E.H.B.; Software, F.B.; Formal analysis, Y.B. (Younes Bahammou) and H.F.; Investigation, Z.T., H.F. and E.H.B.; Data curation, Y.B. (Yassir Bellaziz); Writing—original draft, F.B.; Writing—review & editing, Y.B. (Yassir Bellaziz), Z.T., Y.B. (Younes Bahammou), H.F., E.H.B. and N.O.; Visualization, Z.T., Y.B. (Younes Bahammou) and H.F.; Funding acquisition, N.O. All authors have read and agreed to the published version of the manuscript.

Funding: This research received no external funding.

Institutional Review Board Statement: Not applicable.

Informed Consent Statement: Not applicable.

Data Availability Statement: The data used in the research are described in this article.

Conflicts of Interest: The authors declare that they have no known competing financial interests or personal relationships that could have appeared to influence the work reported in this paper.

Nomenclature

A	Storage bed area (m^2)
C_c	Cover calorific capacity (Jkg^{-1} K^{-1})
C_i	Air calorific capacity (Jkg^{-1} K^{-1})
C_{sl}	Sludge calorific capacity (Jkg^{-1} K^{-1})
$C_{sl\,d}$	Dried sludge calorific capacity (Jkg^{-1} K^{-1})
C_w	Water calorific capacity (Jkg^{-1} K^{-1})
C_r	Rock calorific capacity (Jkg^{-1} K^{-1})
$F_{sl,c}$	Form factor between sludge and cover
$h^r_{sl,c}$	Radiative exchange coefficient between sludge and cover (W m^{-2} K^{-1})
$h^c_{sl,i}$	Convective exchange coefficient between internal air and sludge (W m^{-2} K^{-1})
K_a	Air thermal conductivity (W m^{-1} K^{-1})
L_v	Latent heat of water vaporization (J kg^{-1})
L_c	Characteristic greenhouse length (m)
m_{sl}	Sludge mass (kg)
M_d	Dry sludge mass (kg)
N	Air renewal rate (h^{-1})
Nu	Nusselt Number
S_i	Initial dry solid content of sludge
U	Thermal loss coefficient
S_{sl}	Sludge area (m^2)
S_c	Cover area (m^2)
Q	Heat flux density (W m^{-2})
P	Perimeter of the rock bed (m)
$\dot{m}_{coll}$	Collector mass flow (Kg/s)
$\dot{m}_{rock}$	Rock bed mass flow (kg/s)
T_{coll}	Collector temperature (°C)
T_c	Cover temperature (°C)
T_i	Internal temperature (°C)
T_{sl}	Sludge temperature (°C)
T_{rock}	Rock bed temperature (°C)
U_a	Outdoor air velocity (m s^{-1})
U_i	Internal air velocity (m s^{-1})
V_{gr}	Greenhouse volume (m^3)
T_a	Ambient temperature (°C)
X	Moisture content (kg eau/kg sec)
X_i	Initial moisture content (kg eau/kg sec)
X_r	Reduced moisture content
W_a	Ambient absolute humidity (kg eau/kg sec)
W_i	Absolute internal air humidity (kg eau/kg sec)
α_{sc}, α_{ssl}	Absorption of solar radiation from the cover and sludge
ϵ_c, ϵ_{sl}	Emission of thermal radiation from the cover and sludge
Φ_i	Internal air relative humidity (%)
σ	Stefan–Boltzman Constant(W m^{-2} K^{-4})
ρ	Air density (kg m^{-3})
ρ_r	Rock bed density (kg m^{-3})
c	Cover
sl	Sludge
i	Internal
a	Ambient

References

1. Jin, L.Y.; Zhang, P.Y.; Zhang, G.M.; Li, J. Study of Sludge Moisture Distribution and Dewatering Characteristic after Cationic Polyacrylamide (C-PAM) Conditioning. *Desalination Water Treat.* **2016**, *57*, 29377–29383. [CrossRef]
2. Wu, B.; Dai, X.; Chai, X. Critical review on dewatering of sewage sludge: Influential mechanism, conditioning technologies and implications to sludge re-utilizations. *Water Res.* **2020**, *180*, 115912. [CrossRef]
3. Bennamoun, L. Solar drying of wastewater sludge: A review. *Renew. Sustain. Energy Rev.* **2012**, *16*, 1061–1073. [CrossRef]
4. Ben Hassine, N.; Chesneau, X.; Laatar, A.H. Modelisation and simulation of heat and mass transfers during solar drying of sewage sludge with introduction of real climatic conditions. *J. Appl. Fluid Mech.* **2017**, *10*, 651–659. [CrossRef]
5. Di Fraia, S.; Figaj, R.D.; Massarotti, N.; Vanoli, L. An integrated system for sewage sludge drying through solar energy and a combined heat and power unit fuelled by biogas. *Energy Convers. Manag.* **2018**, *171*, 587–603. [CrossRef]
6. Belloulid, M.O.; Hamdi, H.; Mandi, L.; Ouazzani, N. Solar drying of wastewater sludge: A case study in Marrakesh, Morocco. *Environ. Technol.* **2019**, *40*, 1316–1322. [CrossRef]
7. Kousksou, T.; Allouhi, A.; Belattar, M.; Jamil, A.; El Rhafiki, T.; Arid, A.; Zeraouli, Y. Renewable energy potential and national policy directions for sustainable development in Morocco. *Renew. Sustain. Energy Rev.* **2015**, *47*, 46–57. [CrossRef]
8. Divyangkumar, N.; Sharma, K.; Panwar, N.L.; Saichandhu, G. Sustainability assessment of solar drying systems: A comparative life-cycle analysis of phase-change material-based vs. cylindrical solar dryers. *Clean Energy* **2024**, *8*, 183–196. [CrossRef]
9. Khanlari, A.; Tuncer, A.D.; Sözen, A.; Şirin, C.; Gungor, A. Energetic, environmental and economic analysis of drying municipal sewage sludge with a modified sustainable solar drying system. *Sol. Energy* **2020**, *208*, 787–799. [CrossRef]

10. Gomes, L.A.C.N.; Gonçalves, R.F.; Martins, M.F.; Sogari, C.N. Assessing the suitability of solar dryers applied to wastewater plants: A review. *J. Environ. Manag.* **2023**, *326*, 116640. [CrossRef]
11. Azeddine, F.; El Khadir, L.; Ali, I. Experimental Investigation of Solar Greenhouse Drying of Hydroxide Sludge under Summer and Winter Climate. *Pol. J. Environ. Stud.* **2022**, *31*, 1025–1036. [CrossRef]
12. Masmoudi, A.; Ali, A.B.S.; Dhaouadi, H.; Mhiri, H. Draining solar drying of sewage sludge: Experimental study and modeling. *Environ. Prog. Sustain. Energy* **2021**, *40*, e13499. [CrossRef]
13. Chen, Z.; Hou, Y.; Liu, M.; Zhang, G.; Zhang, K.; Zhang, D.; Yang, L.; Kong, Y.; Du, X. Thermodynamic and economic analyses of sewage sludge resource utilization systems integrating Drying, Incineration, and power generation processes. *Appl. Energy* **2022**, *327*, 120093. [CrossRef]
14. Masmoudi, A.; Sik, A.B.; Dhaouadi, H.; Mhiri, H. Solar drying process for sewage sludge in a drying bed: A case study in Tunisia. *Environ. Prog. Sustain. Energy* **2023**, *42*, e14227. [CrossRef]
15. Svensson, I. Using solar thermal energy in the sludge drying process of a wastewater treatment plant. *AIP Conf. Proc.* **2023**, *2815*, 050004. [CrossRef]
16. Gourdo, L.; Fatnassi, H.; Tiskatine, R.; Wifaya, A.; Demrati, H.; Aharoune, A.; Bouirden, L. Solar energy storing rock-bed to heat an agricultural greenhouse. *Energy* **2019**, *169*, 206–212. [CrossRef]
17. TRNSYS Simulation Studio, TRNSYS 2018, Mathematical Reference T.E.S.S. Available online: https://studylib.net/doc/26018127/trnsys18-%E2%80%93-mathematical-reference (accessed on 10 November 2024).
18. Berroug, F.; Lakhal, E.K.; El Omari, M.E.; Ouazzani, N.; Mandi, L.; Nouh, F.A.; Hejjaj, A.; Bellaziz, Y.; Idlimam, A.; Boukhattem, L. Simulation of sewage sludge drying under climate of solar greenhouse. *AIP Conf. Proc.* **2021**, *2345*, 020044. [CrossRef]
19. Mujumdar, A.S. *Handbook of Industrial Drying*, 4th ed.; CRC Press: Boca Raton, FL, USA, 2014. [CrossRef]
20. Singh, P.; Pandey, B.K.; Gaur, M.K. Performance evaluation of evacuated solar collector assisted hybrid greenhouse solar dryer under active and passive mode. *Mater. Today Proc.* **2022**, *57*, 2002–2008. [CrossRef]
21. Hamdi, I.; Kooli, S.; Elkhadraoui, A.; Azaizia, Z.; Abdelhamid, F.; Guizani, A. Experimental study and numerical modeling for drying grapes under solar greenhouse. *Renew. Energy* **2018**, *127*, 936–946. [CrossRef]
22. Azaizia, Z.; Kooli, S.; Hamdi, I.; Elkhal, W.; Guizani, A.A. Experimental study of a new mixed mode solar greenhouse drying system with and without thermal energy storage for pepper. *Renew. Energy* **2020**, *145*, 1972–1984. [CrossRef]
23. Mujumdar, A.S. Drying principles, classification, and selection of dryers. In *Handbook of Industrial Drying*; CRC Press: Boca Raton, FL, USA, 2014; pp. 4–28.
24. Badaoui, O.; Hanini, S.; Djebli, A.; Haddad, B.; Benhamou, A. Experimental and modelling study of tomato pomace waste drying in a new solar greenhouse: Evaluation of new drying models. *Renew. Energy* **2019**, *133*, 144–155. [CrossRef]
25. Ameri, B.; Hanini, S.; Boumahdi, M. Influence of drying methods on the thermodynamic parameters, effective moisture diffusion and drying rate of wastewater sewage sludge. *Renew. Energy* **2020**, *147*, 1107–1119. [CrossRef]
26. Yu, J.; Chen, L.; Jin, S.; Yan, W. Performance investigation of the double-stage solar air evaporating separation system for saline wastewater treatment. *Desalination* **2021**, *515*, 115194. [CrossRef]
27. Prajapati, S.; Naik, N.; Chandramohan, V.P. Numerical solution of solar air heater with triangular corrugations for indirect solar dryer: Influence of pitch and an optimized pitch of corrugation for enhanced performance. *Sol. Energy* **2022**, *243*, 1–12. [CrossRef]
28. Yu, J.; Yang, J.; Yan, W. Characteristics and performance investigation of solar AES system with novel flat-plate collector-evaporator integrated unit capable of salinity wastewater thermal self-storage. *Desalination* **2023**, *555*, 116559. [CrossRef]